

# Simple, flexible calibration of phase calculation-based three-dimensional imaging system

Zonghua Zhang,<sup>1,3,\*</sup> Haiyan Ma,<sup>1</sup> Tong Guo,<sup>2</sup> Sixiang Zhang,<sup>1</sup> and Jinping Chen<sup>2</sup>

<sup>1</sup>School of Mechanical Engineering, Hebei University of Technology, Tianjin, 300130, China

<sup>2</sup>College of Precision Instrument and Opto-Electronics Engineering, Tianjin University, Tianjin, 300072, China

<sup>3</sup>e-mail: zhzhang@hebut.edu.cn

\*Corresponding author: zhzhangtju@hotmail.com

Received February 14, 2011; revised March 3, 2011; accepted March 4, 2011;  
posted March 8, 2011 (Doc. ID 142663); published March 30, 2011

One important step of phase-based three-dimensional imaging system is calibration, which defines the relationship between phase and depth data. Existing calibration methods are complicated and hard to carry out because of using a translation stage or gauge block in a laboratory environment. This Letter introduces a new simple, flexible calibration method by using a checkerboard and a white plate having discrete markers with known separation. The checkerboard determines the internal parameters of a CCD camera. The plate gives phase and depth data of each pixel to establish their relationship. Experimental results and performance evaluation show that the proposed calibration method can reliably build up the accurate relationship between phase map and depth data in a simple, flexible way. © 2011 Optical Society of America

OCIS codes: 150.6910, 150.1488, 110.6880, 120.2830.

Phase calculation-based fringe projection techniques are active research fields in academia and industry because of the advantages of noncontact operation, full-field acquisition, high accuracy, fast data processing, and low cost [1,2]. Three-dimensional (3D) imaging systems based on such techniques measure the absolute phase corresponding to the 3D shape of an object surface. To obtain the shape of the measured object, the absolute phase needs to be converted into depth data, which is called calibration of 3D imaging systems [3]. Although many calibration methods have been widely studied, it is still challenging to establish the relationship between phase map and depth data using a simple, flexible method for phase-based 3D imaging systems.

Existing calibration methods of 3D systems can be categorized into model based [3,4], polynomial [5,6], and least square [7,8]. All the methods need a translating plate or a 3D standard gauge block. Therefore, existing calibration methods have complicated procedures and only can be performed inside a laboratory environment.

Recently, based on an uneven fringe projection technique, a calibration method was developed using a white plate with discrete markers [9]. This Letter presents a simple, flexible calibration method using a planar checkerboard and a white plate with discrete markers on the surface, as illustrated in Fig. 1. The internal parameters of the system's CCD camera are determined by the checkerboard, while the white plate gives the absolute phase and depth information of each pixel of the captured plate at different positions. Therefore, there are two steps to implement the calibration. Using the general camera calibration procedure [10,11], the first step obtains the internal parameters of the CCD, including two focal lengths ( $F_u$  and  $F_v$ ), two principal point coordinates ( $P_u$  and  $P_v$ ), and four image radial and tangential distortion coefficients ( $K_1$ ,  $K_2$ ,  $K_3$ , and  $K_4$ ). The second step determines the absolute phase and relative depth of each pixel on the white plate surface in the measuring volume. The following describes the details of this calibration technique.

For a general phase calculation-based fringe projection system, because of the crossed optical axes of the imaging and projecting parts, the constant fringe pattern from the projector has variable period on a reference  $M$  perpendicular to the imaging axis, as illustrated in Fig. 2. The relationship between phase map and depth data is a function of the pixel coordinate position of  $x$  and  $y$  and can be represented by the following equation [3]:

$$z = \frac{L_0}{\frac{2\pi L_0^2 L \cos \theta}{P_0 \Delta\varphi(x,y)(L_0+x \cos \theta \sin \theta)^2} - \frac{L \cos \theta \sin \theta}{L_0+x \cos \theta \sin \theta} + 1}, \quad (1)$$

where  $z$  is the depth relative to  $M$ ,  $\Delta\varphi$  is the difference of the unwrapped phase on the measured object and the plane  $M$ ,  $L$  is the baseline between the CCD camera and the digital light processing projector,  $L_0$  is the working distance to  $M$ ,  $\theta$  is the angle between the optical axis of the projector and the camera, and  $P_0$  is the period of the projected fringe pattern on a virtual plane perpendicular to the projecting axis. It is difficult and complicated to directly calibrate the parameters of  $L$ ,  $L_0$ ,  $\theta$ , and  $P_0$ . The proposed calibration method establishes the relationship of phase and depth by a polynomial. In fact, Eq. (1) can be represented by the following polynomial equation:

$$z(x, y) = \sum_{n=0}^N a_n(x, y) \Delta\varphi(x, y)^n, \quad (2)$$

where  $a_n, a_{n-1} \dots a_1, a_0$  are the coefficient set, which contains the systematic parameters. Because of the dependence of Eq. (2) on the  $x$  and  $y$  coordinates, the coefficient set will have different values between pixel positions. Therefore, a look-up table (LUT) should be utilized at each pixel position to save the coefficient set to give highly accurate 3D shape data.

Eight internal parameters of the CCD camera are calibrated by the checkerboard [10,11]. To establish the relationship between phase map and depth data by using an LUT table, the CCD camera is required to capture another series of images of the white plate at different

positions with phase-shifted sinusoidal fringe pattern projected onto the surface. The markers on the plate surface were designed as green hollow rings, as illustrated in Fig. 1(b). On one hand, the position of each marker can be accurately located by an ellipse fitting algorithm [12] from the inner and outer edge of the ring; on the other hand, by projecting green sinusoidal fringe patterns, the modulation of the fringe patterns has high value on the region of the ring so that phase can be obtained at all pixels of the fringe image.

After extracting the inner and outer edges of each hollow ring, the ellipse fitting algorithm calculates the center of the markers, as illustrated in Fig. 3(a). Therefore, the external parameters of the white plate can be determined by the following equation:

$$s[u \ v \ 1]^T = A[R \ T][x_w \ y_w \ z_w \ 1]^T, \quad (3)$$

where  $R$  is a matrix representing the three rotating angles,  $T = [T_x \ T_y \ T_z]$  is a vector representing the three translating distances,  $[x_w \ y_w \ z_w]$  is the coordinate vector of a marker  $P$  on the white plate,  $[u \ v]$  is the coordinate vector of  $P$  in the pixel coordinate system,  $A$  is an internal matrix of the CCD camera (which contains all the obtained internal parameters),  $s$  is an arbitrary scaling factor, and  $[\ ]^T$  denotes the transpose. The camera coordinates  $[x_c \ y_c \ z_c]$  can be expressed as

$$\begin{bmatrix} x_c \\ y_c \\ z_c \end{bmatrix} = \begin{bmatrix} R_{11} & R_{12} & T_x \\ R_{21} & R_{22} & T_y \\ R_{31} & R_{32} & T_z \end{bmatrix} \begin{bmatrix} x_w \\ y_w \\ 1 \end{bmatrix}. \quad (4)$$

The depth  $z$  in Eq. (1) is a relative depth value with regard to the reference plane  $M$ , so the obtained depth  $z_c$  in the camera frame needs to be changed into the reference coordinate system, whose origin is approximately in the middle of the measurement volume. Finally, the relative depth  $z$  of each pixel can be obtained at the plate surface.

At each position of the plate, 12 green sinusoidal fringe patterns having the optimum numbers are sequentially projected onto the plate surface and the deformed fringe patterns are captured by the CCD camera, so the absolute phase of each pixel can be independently calculated by the four-step phase-shifting algorithm plus the optimum three-frequency selection method [13]. Because of the high modulation of the sinusoidal fringe pattern on the green ring, each pixel on the plate, including the re-

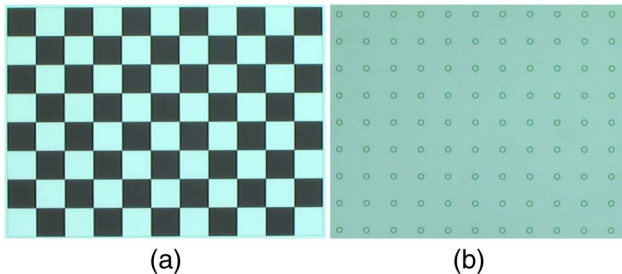


Fig. 1. (Color online) Checkerboard and white plate. (a) Photo of the checkerboard with 15 mm × 15 mm black and white squares, (b) photo of the white plate with 9 × 11 green hollow rings with separation of 15 mm.

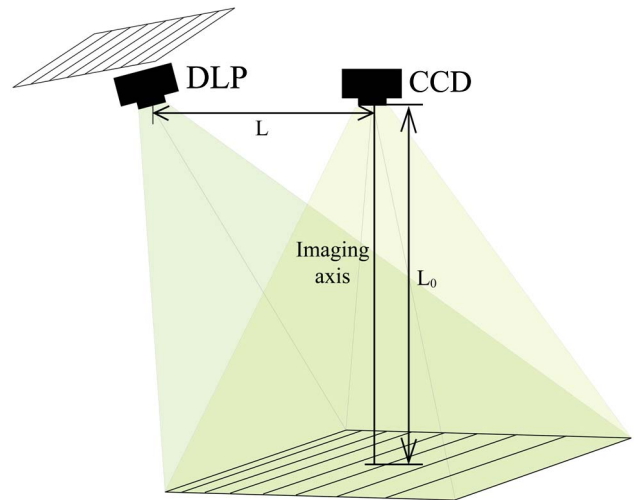


Fig. 2. (Color online) Schematic of even fringe projection at the projector and uneven fringe pattern on the reference  $M$ .  $M$ : reference plane.

gion of markers, can give correct absolute phase information. Figures 3(b) and 3(c) show an image of the white plate with green fringes projected onto it and the corresponding absolute phase map, respectively.

After obtaining the absolute phase and relative depth information of each pixel at all the plate positions, the coefficient set  $a_n, a_{n-1} \dots a_1, a_0$  of Eq. (2) can be calculated by a least-squares method. All the obtained coefficient sets are saved into an LUT table.

A checkerboard having 8 × 11 white and black checkers was manufactured, as illustrated in Fig. 1(a). Each checker has a square size of 15 mm × 15 mm. The board was positioned at eight random positions and orientations with a large angle between the imaging axis and the board's normal. Using the known square size of all the checkers in the eight captured images, the internal parameters of the CCD are obtained by the Camera Calibration Toolbox for Matlab [11]. The radial and tangential distortions of the captured images were corrected by the obtained internal parameters of the CCD camera.

Another white plate having 9 × 11 discrete green hollow ring markers was made, as illustrated in Fig. 1(b). The separation of neighboring markers along row and column direction has the same value of 15 mm. Sixteen positions were randomly chosen with the plate nearly perpendicular to the imaging axis for calibrating the 3D imaging system. At each position, 12 sinusoidal fringe patterns with the optimum numbers of 100, 99, and 90 were projected onto the plate surface for phase calculation, and one image without projected fringe pattern was

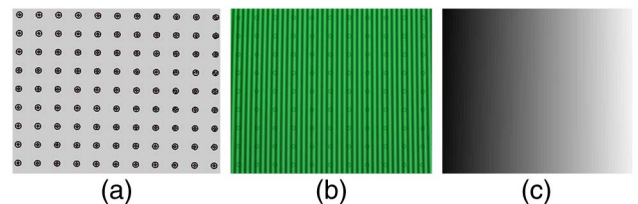


Fig. 3. (Color online) Images on the white plate of calibration. (a) Extracted edge and determined center of 99 circle rings, (b) Deformed fringe pattern on the white plate, and (c) absolute phase map on the plate surface.

captured for marker position determination. An absolute phase map was obtained, as illustrated in Fig. 3(c). The phase data on markers were correctly obtained using the green hollow rings and the green fringe pattern. One can use red or blue hollow rings and the same color fringe pattern to calibrate the system.

From the captured image without projected fringe pattern, the position of each marker center was found by fitting the inner and outer ellipses, as the black dot shown in Fig. 3(a). Using the obtained marker positions and internal parameters, the distance of all the pixels for each plate position to the camera frame is determined by Eq. (4). In order to change the distance into the reference coordinate system, one position in the middle of the measuring volume was chosen as the reference plane  $M$ . A virtual plane, instead of a physical reference plate, was used to reduce the measurement uncertainty. Coefficient set  $a_n, a_{n-1} \dots a_1, a_0$  at each pixel was calculated by the obtained depth and absolute phase data. It was found that a fifth fitting was sufficient to calibrate the system to the level that could be achieved given the available phase resolution.

In order to evaluate the calibrated 3D imaging system, the same plate was placed on a translation stage with

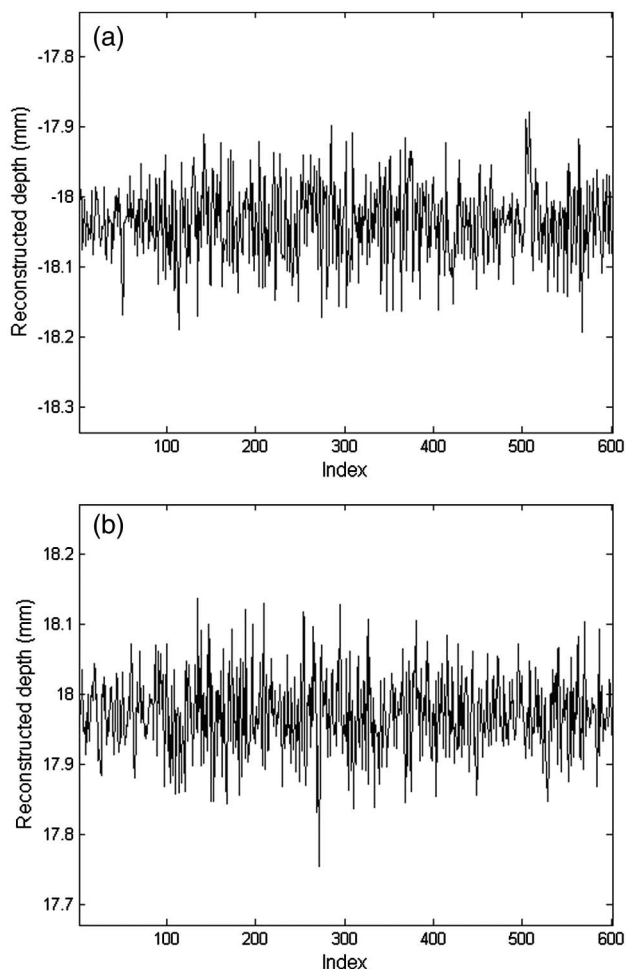


Fig. 4. Measured distance along one row near the middle of the white plate. X axis represents the pixel positions along the row direction with a range 1, 2, 3, ..., 600, the vertical axis is the reconstructed depth of the surface. (a)  $z = -18$  mm, (b)  $z = 18$  mm.

**Table 1. Absolute Error Along the Top, Middle, and Bottom Lines for the Positions  $-18$  mm and  $18$  mm**

Positions	Top	Middle	Bottom
-18	0.044	0.036	0.042
18	0.035	0.023	0.011

resolution of  $10 \mu\text{m}$ . The plate was positioned at  $-18$  and  $18$  mm with respect to the plane  $M$ . The depth data along one row near the middle is illustrated in Fig. 4 for the two positions. At the two positions, the absolute errors are calculated along the top, middle, and bottom lines, as listed in Table 1. The maximum absolute error is  $0.044$  mm. The results show that the proposed calibration method accurately converts the phase into depth data.

In conclusion, a simple, flexible calibration method of phase calculation-based 3D imaging system is introduced by using a checkerboard and a white plate with known separate markers. Since the relationship of each pixel is established by using an LUT table, the proposed calibration method can give highly accurate depth data. The validity and flexibility have been testified by measuring several known depths. Because only a checkerboard and a white plate are required during calibration, this method is easily carried out in actual application fields without limiting one to a laboratory environment. Of course, one can replace the checkerboard with a white plate with known markers to calibrate the internal parameters of a CCD camera.

The authors would like to thank the Scientific Research Foundation for the Returned Overseas Chinese Scholars, State Education Ministry, Research Project supported by Hebei Education Department (under grant ZD2010121), and the National Natural Science Foundation of China (NSFC) (under grant 50975201).

## References

1. F. Chen, G. M. Brown, and M. Song, *Opt. Eng.* **39**, 10 (2000).
2. J. Salvi, S. Fernandez, T. Pribanic, and X. Llado, *Pattern Recogn.* **43**, 2666 (2010).
3. Z. H. Zhang, D. P. Zhang, X. Peng, and X. T. Hu, *Opt. Lasers Eng.* **42**, 341 (2004).
4. Q. Y. Hu, P. S. Huang, Q. L. Fu, and F. P. Chiang, *Opt. Eng.* **42**, 487 (2003).
5. W. S. Li, X. Y. Su, and Z. B. Liu, *Appl. Opt.* **40**, 3326 (2001).
6. P. R. Jia, J. Kofman, and C. English, *Opt. Eng.* **46**, 043601 (2007).
7. M. Vo, Z. Wang, T. Hoang, and D. Nguyen, *Opt. Lett.* **35**, 3192 (2010).
8. L. Huang, P. S. K. Chua, and A. Asundi, *Appl. Opt.* **49**, 1539 (2010).
9. Z. Zhang, H. Ma, S. Zhang, T. Guo, C. E. Towers, and D. P. Towers, *Opt. Lett.* **36**, 627 (2011).
10. Z. Zhang, *IEEE Trans. Pattern Anal. Mach. Intell.* **22**, 1330 (2000).
11. J.-Y. Bouguet, "Camera calibration toolbox for Matlab," [http://www.vision.caltech.edu/bouguetj/calib\\_doc/](http://www.vision.caltech.edu/bouguetj/calib_doc/).
12. A. Fitzgibbon, M. Pilu, and R. B. Fisher, *IEEE Trans. Pattern Anal. Mach. Intell.* **21**, 476 (1999).
13. Z. H. Zhang, C. E. Towers, and D. P. Towers, *Opt. Express* **14**, 6444 (2006).